Structural Engineering and Mechanics, Vol. 46, No. 1 (2013) 111-135
DOI: http://dx.doi.org/10.12989/sem.2013.46.1.111

Strength model for square concrete columns confined by external CFRP sheets

Riad Benzaid*[1] and Habib Abdelhak Mesbah[2a]

[1]*L.G.G., Jijel University-B.P. 98, Cité Ouled Issa, Jijel, 18000, Algeria*
[2]*L.G.C.G.M., INSA of Rennes, University of Rennes 1, France*

(Received January 3, 2012, Revised December 31, 2012, Accepted March 10, 2013)

Abstract. An experimental study has been carried out on square plain concrete (PC) and reinforced concrete (RC) columns strengthened with carbon fiber-reinforced polymer (CFRP) sheets. A total of 78 specimens were loaded to failure in axial compression and investigated in both axial and transverse directions. Slenderness of the columns, number of wrap layers and concrete strength were the test parameters. Compressive stress, axial and hoop strains were recorded to evaluate the stress-strain relationship, ultimate strength and ductility of the specimens. Results clearly demonstrate that composite wrapping can enhance the structural performance of square columns in terms of both maximum strength and ductility. On the basis of the effective lateral confining pressure of composite jacket and the effective FRP strain coefficient, new peak stress equations were proposed to predict the axial strength and corresponding strain of FRP-confined square concrete columns. This model incorporates the effect of the effective circumferential FRP failure strain and the effect of the effective lateral confining pressure. The results show that the predictions of the model agree well with the test data.

Keywords: CFRP; square column; confinement; strength; ductility; slenderness

1. Introduction

During the last decade, the use of FRP composites has been successfully promoted for external confinement of reinforced concrete (RC) columns all over the world. Several studies on the performance of FRP wrapped columns have been conducted, using both experimental and analytical approaches.

Experimental testing was first performed on concrete cylinders wrapped with composites and subjected to uni-axial compression. Saadatmanesh *et al*. (1994) used the stress-strain model proposed by Mander *et al*. (1988) to analyze the behavior of concrete columns externally wrapped with FRP composite straps. The model was used to assess gain in strength and ductility of concrete column confined by FRP materials. Mirmiran *et al*. (1998) discussed how FRP materials significantly enhance the strength, ductility and durability of concrete columns. The longitudinal fibers serve as flexural reinforcement, while hoop fibers provided confinement and shear strength. Samaan *et al*. (1998) developed a confinement model for FRP-confined concrete applicable to

*Corresponding author, Associate Professor, E-mail: benzaid_riad@yahoo.fr
[a]Associate Professor, E-mail: habib-abdelhak.mesbah@univ-rennes1.fr

circular sections only. The model predicts the entire stress–strain curve of FRP-confined concrete in both, the axial and lateral directions. Rochette and Labossière (2000) studied the behaviors of prisms confined with carbon and aramid fiber sheets tested under uni-axial compression. Their tests quantified the influence of some parameters including confinement stiffness and corner radius on the stress-strain response of FRP-confined concrete prisms. Shehata *et al*. (2002) proposed empirical equations to calculate the confinement concrete strength and the ultimate confined concrete strain as a function of the confining lateral stress for circular, square and rectangular columns. Campione and Miraglia (2003) proposed an analytical model to evaluate the confining pressure in ultimate conditions considering the effective confined cross-section and also allow one to determine the ultimate strain corresponding to FRP failure through a simplified energetic approach. Wu *et al*. (2006) developed a confinement models applicable to circular sections only, a boundary value is given to differentiate between strain softening and strain hardening responses of FRP-confined concrete. Besides, for the case of FRP-confined concrete cylinders with a strain-softening response, equations for predicting the maximum strength, peak strain, ultimate strength and ultimate strain are proposed. Almusallam (2007) showed experimentally that the compressive strength and ductility of the concrete cylinders increases with number of composite layers and effect of confinement is substantial for normal strength concrete and marginal for high-strength concrete. A semi-empirical theoretical model is also proposed in order to predict stress-strain relationship of GFRP confined concrete cylinders. Benzaid *et al*. (2010) proposed a simple model to predict the compressive strength and axial strain of circular FRP-confined columns. This model incorporates the effect of the effective circumferential FRP failure strain.

Most of the available studies on the behavior of FRP confined concrete columns have concentrated on circular shaped columns with normal strength. However, the vast majority of all columns in buildings are square or rectangular columns. The data available for columns of square or rectangular cross sections have increased over recent years but are still limited. Also the validation of these results and their applicability to large-scale RC columns is of great practical interest. This field remains in its developmental stages and more research investigation is needed on this subject to study the effect of slenderness and that of concrete strength.

Shapes of cross-sections of columns can directly affect the confinement effectiveness of externally bonded FRP jackets. Benefit of strength is higher for circular than for square or rectangular sections. Poor confinement may be due to concentration of stresses at the corner of the specimens and consequently to the lower confining pressure and smaller effective concrete core area. Yang *et al*. (2001) studied effect of corner radius on the performance of externally bonded FRP reinforcement. They observed that as the corner radius decreases efficiency of FRP wrapping also decreases. Cole and Belarbi (2001) investigated the effectiveness of FRP confinement on rectangular RC columns. They studied experimentally effects of: - fibers type; thickness of FRP jacket; - the aspect ratio of the rectangular cross section and the radius of the corners; on the axial strength and axial strain of rectangular RC column subjected to uni-axial compression. They observed that an increase in the sharpness of the corners of the cross section results in a lower ultimate strength and an increase in the aspect ratio of the cross section results in a lower ultimate strength. Benzaid *et al*. (2008, 2009) showed experimentally that for FRP wrapped concrete columns the strength and ductility gains increase with the radius of the columns corner. They observed that: - the efficiency of the confinement was very sensitive to the specimen cross section geometry and the confining stress expressed in the number of the FRP sheet layers applied; - the best performance was that of the circular specimens followed by the square specimens having corners radius of 16 mm, 8 mm, than 0 mm corners radius, respectively. This is attributed to the

fact that a jacket delivers a uniform confining stress around the circular concrete core and to the intensification of stresses at the corners of square specimens.

This study deals with a series of tests on square plain concrete (PC) and reinforced concrete (RC) columns strengthened with CFRP sheets. A total of 78 concrete specimens were tested under axial compression. The data recorded included the compressive loads, axial strains, and radial strains. The parameters considered are the number of composite layers (1 and 3), the compressive strength of the unconfined concrete (26, 50 and 62 MPa) and the columns' slenderness ratio L/a (2; 4 and 7.14). To comply with existing RC members in practice, where reduced cover is often present, the corners for all prismatic specimens were almost kept sharp for CFRP application.

2. Research significance

In existing models for FRP-confined concrete, it is commonly assumed that the FRP ruptures when the hoop stress in the FRP jacket reaches its tensile strength from either flat coupon tests which is herein referred to as the FRP material tensile strength. This assumption is the basis for calculating the maximum confining pressure f_l (the confining pressure reached when the FRP ruptures) given by Eq. (1). However, according to the obtained test results, specimen failure occurs before the FRP reached their ultimate strain capacities. So the failure occurs prematurely and the circumferential failure strain was lower than the ultimate strain obtained from standard tensile testing of the FRP composite. This phenomenon considerably affects the accuracy of the existing models for FRP-confined concrete. This reduction in the strain of the FRP composites can be attributed to several causes as reported in related literature (Matthys *et al*. 2005, Benzaid *et al*. 2009):

- The curved shape of the composite wrap or misalignment of fibers may reduce the FRP axial strength;
- Near failure the concrete is internally cracked resulting in non-homogeneous deformations. Due to this non-homogeneous deformations and high loads applied on the cracked concrete, local stress concentrations may occur in the FRP reinforcement.
- Concentration of stresses at the corner of the square or rectangular specimens

This article is directed towards this endeavor. A simple model is proposed in order to predict the axial strength and corresponding strain of FRP-confined square concrete columns. This model incorporates the effect of the effective circumferential FRP failure strain and the effect of the effective lateral confining pressure.

3. FRP confinement of concrete

The confinement of concrete with FRP is based on a well-understood mechanism. The confinement action exerted by the FRP on the concrete core is of the passive type, that is, it arises as a result of the lateral expansion of concrete under axial load. When the concrete is subjected to axial compression, it expands laterally. This expansion is resisted by the FRP jacket which provides a confining pressure to the concrete. Concrete in a circular jacket is uniformly confined, while concrete in a jacket of any other sectional shape is non-uniformly confined.

3.1 FRP-confined concrete in square columns

A square column confined with FRP composite is shown in Fig. 1. To improve the effectiveness of FRP confinement, corner rounding is generally recommended. Existing researches on steel confined concrete (Park and Paulay 1975, Mander *et al*. 1988, Cusson and Paultre 1995) have led to the simple proposition that the concrete in a square section is confined by the transverse reinforcement through arching actions, and only the concrete contained by the four second-degree parabolas as shown in Fig. 1(a) is fully confined while the confinement to the rest is negligible. While there are differences between steel and FRP in providing confinement, the observation that only part of the section is well confined is obviously also valid in the case of FRP confinement (Lam and Teng 2003). Youssef *et al*. (2007) showed that confining square concrete members with FRP materials tends to produce confining stress concentrated around the corners of such members, as shown in Fig. 1(b). The reduced effectiveness of an FRP jacket for a square section than for a circular section has been confirmed by experimental results (Mirmiran *et al*. 1998, Rochette and Labossière 2000). Despite this reduced effectiveness, an FRP-confined square concrete column generally also fails by FRP rupture (Rochette and Labossière 2000, Benzaid *et al*. 2008).

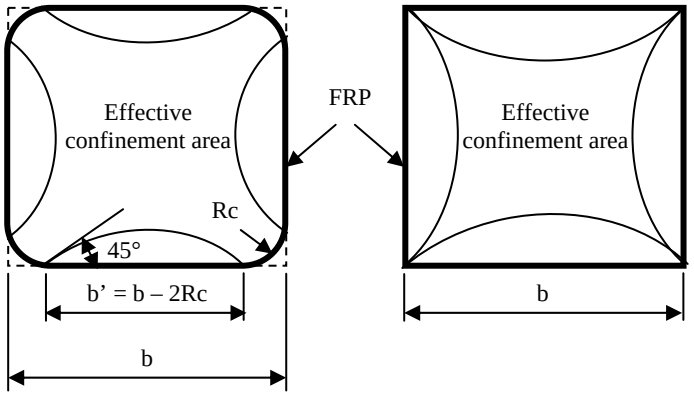

(a) Effectively confined concrete in a square column

(b) Dilated square column confined with carbon/epoxy jacket (Youssef *et al*. 2007)

Fig. 1 Confinement action of FRP composite in square sections

For circular columns, the concrete is subject to uniform confinement, and the maximum confining pressure provided by FRP composite is related to the amount and strength of FRP and the diameter of the confined concrete core. The maximum value of the confinement pressure that the FRP can exert is attained when the circumferential strain in the FRP reaches its ultimate strain. This confining pressure is given by Lam and Teng (2003), Al-Salloum (2007), Benzaid *et al*. (2010)

$$f_l = \frac{2\ t_{frp}\ E_{frp}\ \varepsilon_{fu}}{d} = \frac{2\ t_{frp}\ f_{frp}}{d} = \frac{\rho_{frp}\ f_{frp}}{2} \tag{1}$$

Where f_l is the lateral confining pressure, E_{frp} is the elastic modulus of the FRP composite, ε_{fu} is the ultimate FRP tensile strain, f_{frp} is the ultimate tensile strength of the FRP composite, t_{frp} is the total thickness of the FRP, d is the diameter of the concrete column, and ρ_{frp} is the FRP volumetric ratio.

In Eq. (1), d is replaced by the diagonal length of the square section. For a square section with rounded corners, d can be written as Al-Salloum (2007)

$$d = \sqrt{2}\, b - 2\,\mathrm{Rc}\,(\sqrt{2}\,-1) \tag{2}$$

It should be noted that due to the non-uniformity of confinement in a square section, for a given axial strain, the stress sustained by the concrete varies over the section. The commonly accepted approach is to define the stress as the average axial stress.

4. Experimental program

4.1 Materials properties

Three kind of concrete mix have been realized to investigate the influence of concrete strength as indicated in Table 1. The three categories represent normal strength concrete (NSC, f'_{co} = 26 MPa), medium strength concrete (MSC, f'_{co} = 50 MPa) and high strength concrete (HSC, f'_{co} = 62 MPa).

The carbon-fiber sheets used in this study were the SikaWrap-230C/45 product, a unidirectional wrap. The resin system that was used to bond the carbon fabrics over the specimens in this work was the epoxy resin made of two-parts, resin and hardener. The mixing ratio of the two components by weight was 4:1. SikaWrap-230C/45 was field laminated using Sikadur-330 epoxy to form a carbon fiber reinforced polymer wrap (CFRP) used to strengthen the concrete specimens.

Table 1 Concrete mixture proportions

Mixture no.	I	II	III
Compressive cylinder strength, f'_{co} (MPa)	25.93	49.46	61.81
Cement (kg/m^3)	280[a]	400[b]	450[c]
Water (kg/m^3)	180	183.86	170
Crushed gravel (kg/m^3)			
Ø 4/6	122.90	115.70	115.60
Ø 6/12	258.20	243.00	242.80
Ø 12/20	769.50	724.20	723.50
Sand Ø 0/4 (kg/m^3)	729.10	686.30	685.60
Sika Viscocrete-Tempo12 (l/ m^3), [d]	-	0.85	1.55
Air content (%)	2.3	2.5	2.7
W/C	0.64	0.46	0.37

[a]Portland cement: CPA CEM II R 32.5 MPa.
[b]Portland cement: CPA CEM I R 42.5 MPa.
[c]Portland cement: CPA CEM I R 52.5 MPa.
[d]Sika Viscocrete-Tempo 12: High-range water reducing and super-plasticizing admixture.

The mechanical properties, including the modulus and the tensile strength of the CFRP composite, were obtained through tensile testing of flat coupons. The relevant test method is described in NF EN ISO 527-(1, 2 and 5). The tensile specimen configuration is represented in Fig. 2. Main mechanical properties obtained from the average values of the tested coupons are summarized in Table 2. Note that the tensile strength was defined based on the cross-sectional area of the coupons, while the elastic modulus was calculated from the stress-strain response.

This research work was carried out in the Department of Civil Engineering laboratory (I.U.T University of Rennes 1- France). Nine series of experiments were performed to investigate the behavior of plain- and reinforced concrete square columns confined by CFRP composite. Table 3 summarizes the specimens involved in the experimental program. For all reinforced concrete specimens the diameter of longitudinal and transverse reinforcing steel bars were respectively 12 mm and 8 mm. The longitudinal steel ratio was constant for all specimens and equal to 2.30 %.The yield strength of the longitudinal and transversal reinforcement was 500 MPa and 235 MPa; respectively.

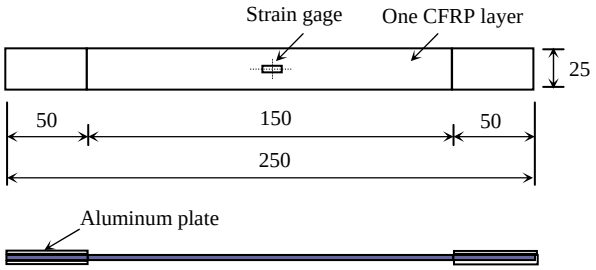

Fig. 2 Dimensions of CFRP flat coupons

Table 2 Properties of the CFRP composite

Thickness (per ply)	1 mm
Modulus E_{frp}	34 GPa
Tensile strength f_{frp}	450 MPa
Ultimate strain ε_{fu}	14 ‰

Table 3 Details of test specimens

Specimen designation	Concrete mixture	Nominal dimensions (diameter x height) [mm]	Number of CFRP layers	Number of specimens	Unconfined concrete strength [MPa]
SPCI.x.0L	I	140x140x280	0	2	26
SPCI.x.1L			1	1	
SPCI.x.3L			3	1	
SRCI.x.0L			0	2	
SRCI.x.1L			1	2	
SRCI.x.3L			3	2	

Table 3 Continued

SPCI.y.0L	I	140x140x560	0	2	26
SPCI.y.1L			1	1	
SPCI.y.3L			3	1	
SRCI.y.0L			0	2	
SRCI.y.1L			1	2	
SRCI.y.3L			3	2	
SRCI.z.0L		140x140x100	0	2	
SRCI.z.1L			1	2	
SRCI.z.3L			3	2	
SPCII.x.0L	II	140x140x280	0	2	50
SPCII.x.1L			1	1	
SPCII.x.3L			3	1	
SRCII.x.0L			0	2	
SRCII.x.1L			1	2	
SRCII.x.3L			3	2	
SPCII.y.0L		140x140x560	0	2	
SPCII.y.1L			1	1	
SPCII.y.3L			3	1	
SRCII.y.0L			0	2	
SRCII.y.1L			1	2	
SRCII.y.3L			3	2	
SRCII.z.0L		140x140x100	0	2	
SRCII.z.1L			1	2	
SRCII.z.3L			3	2	
SPCIII.x.0L	III	140x140x280	0	2	62
SPCIII.x.1L			1	1	
SPCIII.x.3L			3	1	
SRCIII.x.0L			0	2	
SRCIII.x.1L			1	2	
SRCIII.x.3L			3	2	
SPCIII.y.0L		140x140x560	0	2	
SPCIII.y.1L			1	1	
SPCIII.y.3L			3	1	
SRCIII.y.0L			0	2	
SRCIII.y.1L			1	2	
SRCIII.y.3L			3	2	
SPCIII.z.0L		140x140x100	0	2	
SPCIII.z.1L			1	2	
SPCIII.z.3L			3	2	

The specimen notations are as follows. The first letter refers to section shape: S for square, the next two letters refer to the type of concrete: PC for plain concrete and RC for reinforced concrete, followed by the concrete mixture: I for normal strength (26 MPa), II for medium strength (50

MPa) and III for high strength (62 MPa). The next letter indicates the slenderness ratio: x for L/a = 2, y for L/a = 4 and z for L/a = 7.14. The last letters specifies the number of CFRP layers (0L, 1L and 3L), followed by the number of specimen.

4.2 Specimen preparation

After concrete columns were fully cured, FRP wrapping procedure was performed according to the procedure specified by the manufacturer. The CFRP jackets were applied to the specimens by manual wet lay-up process. The concrete specimens were cleaned and completely dried before the resin was applied. The epoxy resin was directly applied onto the substrate. The fabric was carefully placed into the resin with gloved hands and smooth out any irregularities or air pockets using a plastic laminating roller. The roller was continuously used until the resin was reflected on the surface of the fabric, an indication of fully wetting. A second layer of resin was applied to allow the impregnation of the CFRP. The following layer is applied in the same way. Finally, a layer of resin was applied to complete the operation. The last CFRP layer was wrapped around the specimen with an overlap of 1/4 of the perimeter to avoid sliding or deboning of fibers during tests. The wrapped specimens were left at room temperature for 1 week before testing. Fig. 3 shows samples of the wrapped specimens.

4.3 Test procedure

Specimens were loaded under a monotonic uni-axial compression load up to failure. The load was applied at a rate corresponding to 0.24 MPa/s and was recorded with an automatic data acquisition system. Axial and lateral strains were measured using appreciable extensometer. The instrumentation included one lateral linear variable differential transducer (LVDT) placed in the form of a square frame at the mid-height of the specimens. Measurement devices also included three vertical LVDTs to measure the average axial strains. Prior to testing, all CFRP-wrapped specimens were capped with sulfur mortar at both ends. The test setup for the various specimens is shown in Fig. 4.

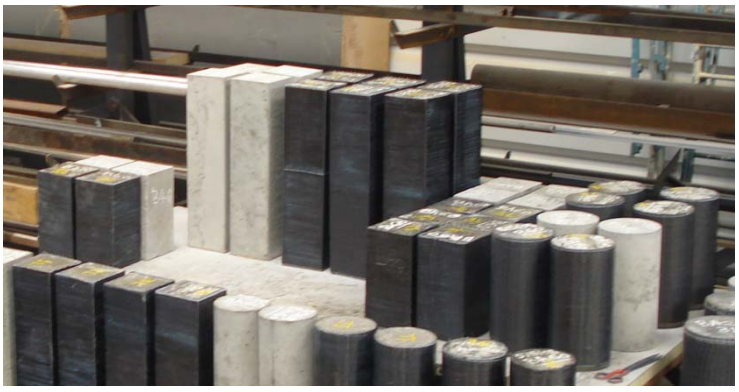

Fig. 3 Samples of specimens after curing and wrapping

5. Test results and discussion

Compression behavior of the CFRP wrapped specimens was mostly similar in each series in terms of stress-strain curves and failure modes of the specimens. All confined concrete columns failed by fracture of the composite wrap at one of the corners, because of the high stress concentration at these locations, as shown in Fig. 5. The collapse occurred in a sudden and explosive way, though some popping noises were heard during various stages of loading and were attributed to micro-cracking of the concrete. The strain values observed for the jacket tensile failure were quite lower than the FRP failure strain.

For short specimens (L/a = 2), the fiber rupture starts mainly in their central zone, then propagates towards both ends. Regarding slender specimens (L/a = 4 or 7.14), the collapse was mostly concentrated in their end regions, indicating that the greater the slender ratio, the smaller the area of CFRP ruptured (Fig. 5). For these columns at ultimate load, when confinement action was no longer provided due to FRP fracture, the internal steel started buckling and the crushed concrete fell down between the fractured FRP. Hence, this indicates that the concrete core is significantly damaged (but yet confined) even before reaching ultimate load. For all confined specimens, delamination was not observed at the overlap location of the CFRP jacket, which confirmed the adequate stress transfer over the splice.

The average experimental results are reported in Tables 4, 5 and 6, with the increase in terms of compressive strength (f'_{cc}/f'_{co}) and ductility ($\varepsilon_{cc}/\varepsilon_{co}$), intended as ultimate axial displacement.

(140x140x280) (140x140x560) mm (140x140x1000)

Fig. 4 Test setup

SRCI.x.3L_1 SRCII.x.3L_1 SRCIII.x.3L_1

SRCI.y.3L_1 SRCII.y.1L_1 SRCIII.y.1L_1

SRCI.z.1L_1 SRCII.z.1L_1 SRCIII.z.3L_1

Fig. 5 Typical failure modes for the tested CFRP-confined columns

Table 4 Experimental results of CFRP-wrapped specimens (140x140x280 mm)

Specimen Code	f'_{cc} [MPa]	f'_{cc} (average) [MPa]	f'_{cc}/f'_{co}	ε_{cc} [‰]	ε_{cc} (average) [‰]	$\varepsilon_{cc}/\varepsilon_{co}$	$\varepsilon_{h,rup}$ [‰]	$\varepsilon_{h,rup}$ (average) [‰]	$\varepsilon_{h,rup}/\varepsilon_{ho}$
SPCI.x.0L$_1$	24,57	24,77	**1,00**	1,69	2,17	**1,00**	3,42	3,62	**1,00**
SPCI.x.0L$_2$	24,98			2,66			3,82		
SPCI.x.1L$_1$	27,66	27,66	**1,11**	5,58	5,58	**2,57**	12,23	12,23	**3,37**
SPCI.x.3L$_1$	32,03	32,03	**1,29**	6,05	6,05	**2,78**	13,23	13,23	**3,65**
SRCI.x.0L$_1$	33,39	33,59	**1,00**	4,22	4,29	**1,00**	8,74	9,38	**1,00**
SRCI.x.0L$_2$	33,80			4,36			10,03		
SRCI.x.1L$_1$	40,48	41,02	**1,20**	5,36	6,08	**1,24**	10,28	11,58	**1,09**
SRCI.x.1L$_2$	41,56		**1,23**	6,80		**1,58**	12,88		**1,37**
SRCI.x.3L$_1$	48,82	49,12	**1,45**	8,98	8,40	**2,09**	13,47	14,38	**1,43**
SRCI.x.3L$_2$	49,42		**1,47**	7,83		**1,82**	15,30		**1,63**
SPCII.x.0L$_1$	47,65	48,53	**1,00**	3,53	3,38	**1,00**	3,90	3,83	**1,00**
SPCII.x.0L$_2$	49,41			3,24			3,77		
SPCII.x.1L$_1$	52,52	52,52	**1,08**	4,03	4,03	**1,19**	7,34	7,34	**1,91**
SPCII.x.3L$_1$	58,25	58,25	**1,20**	6,72	6,72	**1,98**	9,88	9,88	**2,57**
SRCII.x.0L$_1$	52,24	52,82	**1,00**	3,19	4,07	**1,00**	6,02	7,50	**1,00**
SRCII.x.0L$_2$	53,40			4,96			8,98		
SRCII.x.1L$_1$	63,43	62,04	**1,20**	4,34	5,41	**1,06**	7,60	8,56	**1,01**
SRCII.x.1L$_2$	60,66		**1,14**	6,49		**1,59**	9,53		**1,27**
SRCII.x.3L$_1$	67,37	69,09	**1,27**	7,77	6,89	**1,90**	11,56	10,83	**1,54**
SRCII.x.3L$_2$	70,81		**1,34**	6,01		**1,47**	10,11		**1,34**
SPCIII.x.0L$_1$	60,24	59,53	**1,00**	3,66	3,56	**1,00**	4,06	3,89	**1,00**
SPCIII.x.0L$_2$	58,82			3,46			3,73		
SPCIII.x.1L$_1$	61,30	61,30	**1,02**	3,69	3,69	**1,03**	3,97	3,97	**1,02**
SPCIII.x.3L$_1$	70,35	70,35	**1,18**	4,94	4,94	**1,38**	6,69	6,69	**1,71**
SRCIII.x.0L$_1$	63,82	63,79	**1,00**	3,82	3,75	**1,00**	6,08	5,71	**1,00**
SRCIII.x.0L$_2$	63,76			3,68			5,34		
SRCIII.x.1L$_1$	72,86	74,84	**1,14**	3,85	3,87	**1,02**	5,78	5,74	**1,01**
SRCIII.x.1L$_2$	76,82		**1,20**	3,89		**1,03**	5,71		**1,00**
SRCIII.x.3L$_1$	79,58	79,59	**1,24**	5,02	5,14	**1,33**	7,16	7,96	**1,25**
SRCIII.x.3L$_2$	79,60		**1,24**	5,26		**1,40**	8,76		**1,53**

Table 5 Experimental results of CFRP-wrapped specimens (140x140x560 mm)

Specimen Code	f'_{cc} [MPa]	f'_{cc} (average) [MPa]	f'_{cc}/f'_{co}	ε_{cc} [‰]	ε_{cc} (average) [‰]	$\varepsilon_{cc}/\varepsilon_{co}$	$\varepsilon_{h,rup}$ [‰]	$\varepsilon_{h,rup}$ (average) [‰]	$\varepsilon_{h,rup}/\varepsilon_{ho}$
SPCI.y.0L_1	24,95	24,37	**1,00**	1,25	1,12	**1,00**	1,27	1,23	**1,00**
SPCI.y.0L_2	23,80			1,00			1,20		
SPCI.y.1L_1	28,80	28,80	**1,18**	1,89	1,89	**1,68**	2,56	2,56	**2,08**
SPCI.y.3L_1	31,92	31,92	**1,31**	2,89	2,89	**2,58**	5,16	5,16	**4,19**
SRCI.y.0L_1	30,65	30,49	**1,00**	1,71	1,77	**1,00**	2,06	2,44	**1,00**
SRCI.y.0L_2	30,33			1,84			2,82		
SRCI.y.1L_1	35,72	36,73	**1,17**	2,50	2,77	**1,41**	4,39	4,42	**1,79**
SRCI.y.1L_2	37,74		**1,23**	3,04		**1,71**	4,45		**1,82**
SRCI.y.3L_1	41,39	41,85	**1,35**	4,32	4,40	**2,44**	9,43	9,95	**3,86**
SRCI.y.3L_2	42,32		**1,38**	4,48		**2,53**	10,47		**4,29**
SPCII.y.0L_1	44,58	46,66	**1,00**	1,49	1,43	**1,00**	0,24	0,25	**1,00**
SPCII.y.0L_2	48,74			1,38			0,26		
SPCII.y.1L_1	50,74	50,74	**1,08**	2,08	2,08	**1,45**	0,50	0,50	**2,00**
SPCII.y.3L_1	54,12	54,12	**1,16**	2,76	2,76	**1,93**	0,98	0,98	**3,92**
SRCII.y.0L_1	52,83	52,67	**1,00**	2,07	2,11	**1,00**	0,43	0,43	**1,00**
SRCII.y.0L_2	52,52			2,16			0,43		
SRCII.y.1L_1	61,84	61,61	**1,17**	2,89	2,92	**1,36**	0,78	0,73	**1,81**
SRCII.y.1L_2	61,39		**1,16**	2,96		**1,40**	0,68		**1,58**
SRCII.y.3L_1	67,14	65,91	**1,27**	3,23	3,26	**1,53**	1,31	1,37	**3,04**
SRCII.y.3L_2	64,68		**1,22**	3,30		**1,56**	1,43		**3,32**
SPCIII.y.0L_1	59,72	58,60	**1,00**	2,26	1,98	**1,00**	0,57	0,59	**1,00**
SPCIII.y.0L_2	57,48			1,70			0,62		
SPCIII.y.1L_1	62,34	62,34	**1,06**	2,70	2,70	**1,36**	0,82	0,82	**1,38**
SPCIII.y.3L_1	64,66	64,66	**1,10**	2,88	2,88	**1,45**	1,30	1,30	**2,20**
SRCIII.y.0L_1	63,01	63,62	**1,00**	2,16	2,08	**1,00**	0,39	0,35	**1,00**
SRCIII.y.0L_2	64,23			2,00			0,32		
SRCIII.y.1L_1	72,03	72,78	**1,13**	2,82	2,82	**1,35**	0,40	0,45	**1,14**
SRCIII.y.1L_2	73,54		**1,15**	2,82		**1,35**	0,50		**1,42**
SRCIII.y.3L_1	77,39	77,94	**1,21**	2,92	2,94	**1,40**	0,80	0,76	**2,28**
SRCIII.y.3L_2	78,49		**1,23**	2,97		**1,42**	0,72		**2,05**

Table 6 Experimental results of CFRP-wrapped specimens (140x140x1000 mm)

Specimen Code	f'_{cc} [MPa]	f'_{cc} (average) [MPa]	f'_{cc}/f'_{co}	ε_{cc} [‰]	ε_{cc} (average) [‰]	$\varepsilon_{cc}/\varepsilon_{co}$	$\varepsilon_{h,rup}$ [‰]	$\varepsilon_{h,rup}$ (average) [‰]	$\varepsilon_{h,rup}/\varepsilon_{ho}$
SRCI.z.0L$_1$	24,94	24,69	**1,00**	1,09	0,96	**1,00**	-	-	-
SRCI.z.0L$_2$	24,45			0,84			-		
SRCI.z.1L$_1$	33,16	33,92	**1,34**	1,81	2,05	**1,88**	-	-	-
SRCI.z.1L$_2$	34,69		**1,40**	2,30		**2,39**	-		-
SRCI.z.3L$_1$	39,82	39,17	**1,61**	4,27	3,64	**4,44**	-	-	-
SRCI.z.3L$_2$	38,52		**1,56**	3,02		**3,14**	-		-
SRCII.z.0L$_1$	53,23	48,26	**1,00**	1,57	1,38	**1,00**	0,28	0,30	**1,00**
SRCII.z.0L$_2$	43,29			1,20			0,32		
SRCII.z.1L$_1$	60,17	60,16	**1,24**	1,86	1,88	**1,34**	0,61	0,66	**2,03**
SRCII.z.1L$_2$	60,15		**1,24**	1,90		**1,37**	0,72		**2,40**
SRCII.z.3L$_1$	65,60	65,71	**1,35**	3,16	2,86	**2,28**	0,88	0,86	**2,93**
SRCII.z.3L$_2$	65,82		**1,36**	2,56		**1,85**	0,84		**2,80**
SRCIII.z.0L$_1$	61,83	60,98	**1,00**	2,09	2,08	**1,00**	0,55	0,49	**1,00**
SRCIII.z.0L$_2$	60,14			2,08			0,43		
SRCIII.z.1L$_1$	65,76	66,77	**1,07**	1,90	2,13	**0,91**	0,64	0,82	**1,30**
SRCIII.z.1L$_2$	67,78		**1,11**	2,37		**1,13**	1,00		**2,04**
SRCIII.z.3L$_1$	72,52	72,51	**1,18**	3,87	4,10	**1,86**	1,31	1,36	**2,67**
SRCIII.z.3L$_2$	72,50		**1,18**	4,34		**2,08**	1,42		**2,89**

5.1 Stress-strain response

Representative stress-strain curves for each series of tested CFRP-wrapped specimens are reported in Figs. 6 (a-c) for NSC, Figs. 7 (a-c) for MSC and in Figs. 8 (a-c) for HSC. These figures give the axial stress versus the axial and lateral strains for specimens with 0, 1 and 3 layers of CFRP wrap considering various slenderness ratio L/a (2, 4 and 7.14).

For NSC, all CFRP strengthened specimens showed a typical bilinear trend with a transition zone. Three zones can be observed for the stress-strain curves of the CFRP-confined specimens. The first zone is essentially a linear response governed by the stiffness of the unconfined concrete, which indicates that no confinement is activated in the CFRP wraps since the lateral strains in the concrete are very small. The unconfined concrete specimens show a sudden drop in stiffness and strength after reaching the maximum load point. In the second zone, a nonlinear transition occurs as the concrete expands, thus producing larger lateral strains. The CFRP wrap reacts accordingly and a confining action is created on the concrete core. During this stage a loss of stiffness occurs due to the rapidly growing network of cracks in the concrete. Finally, in the third zone, the concrete is fully cracked and the CFRP confinement is activated to provide additional load carrying capacity by keeping the concrete core intact. The stress-strain curve here increases up to failure. However, no distinct post behavior is observed for specimens with higher slenderness ratio.

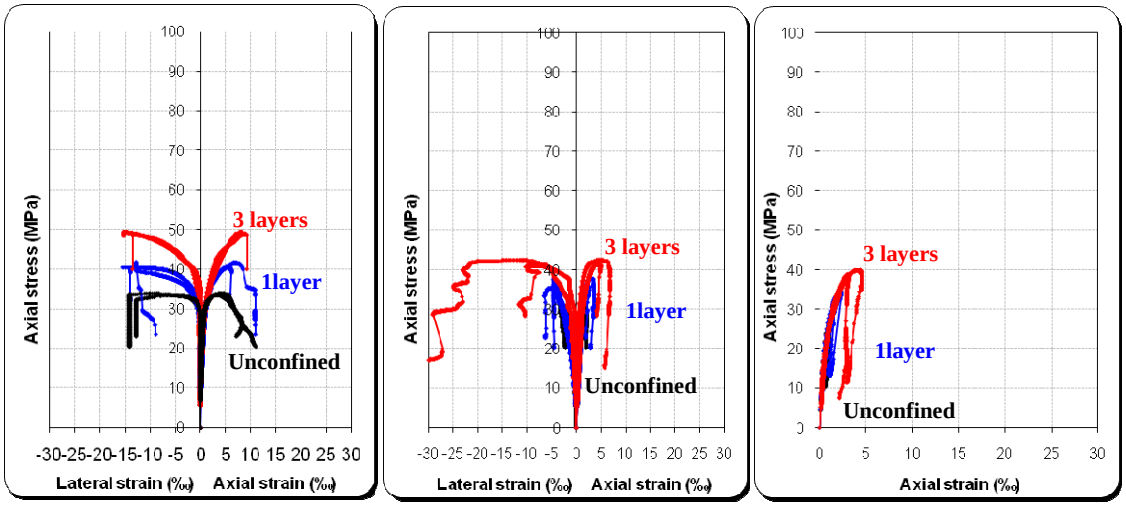

(a) SRCI.x series (b) SRCI.y series (c) SRCI.z series

Fig. 6 Stress strain curves of NSC CFRP confined specimens

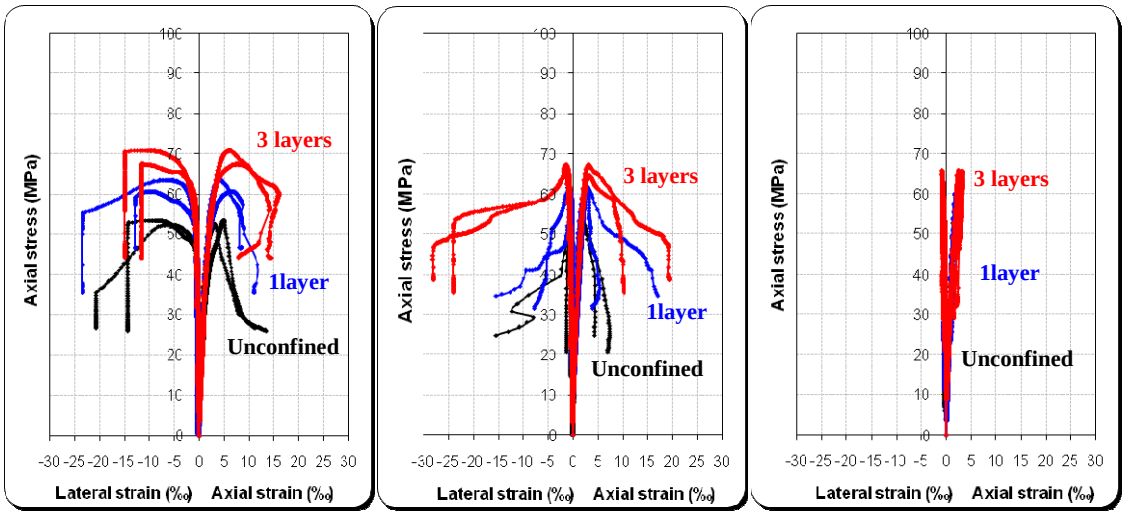

(a) RCII.x series (b) RCII.y series (c) RCII.z series

Fig. 7 Stress strain curves of MSC CFRP-confined specimens

As for the previous case of NSC, the first slope of the curve, regarding specimens with MSC and HSC, is also not substantially altered by the presence of CFRP. In this initial elastic zone, the confined and the unconfined specimens behave in the same manner, irrespective of the number of layers. The strengthening effect of the CFRP layers begins only after the concrete has reached the peak strength of the unconfined concrete: transversal strains in the concrete activate the CFRP jacket. The stress-strain curve features a post-peak descending branch and the compressive strength is reached before FRP rupture. This decreasing type of stress-strain curves can be further differentiated in terms of the stress in concrete at the ultimate strain f'_{cu}. If the stress-strain curve terminates at a concrete stress f'_{cu} above the compressive strength of unconfined concrete f'_{co}, the

FRP confinement is still sufficient to lead to strength enhancement. Such concrete is also referred to as sufficiently confined concrete. However, if the stress-strain curve terminates at a stress $f'_{cu} < f'_{co}$, the specimen is said to be insufficiently confined, where little strength enhancement can be expected. Such insufficiently-confined concrete should not be allowed in design.

5.2 Effect of the numbers of CFRP layers

In all cases the increase of the numbers of CFRP layers generated an increase of compressive strength as well as axial deformation capacity (Figs. 6, 7 and 8). The level of increase is important for NSC specimens. Considering the cases of RC specimens confined with 1 and 3 CFRP layers, from results displayed in Tables 4, 5 and 6 it can be evaluated that the increase in the axial strength varies on average roughly from 20 % to 58 % as compared to the relative unconfined specimens, while the axial strain at peak stress increase on average from 41 % to 279 %. From these findings, it is possible to assert that the increase in the number of CFRP sheets has a significant influence even though the increase in terms of strength is not as important as that of axial strain which increase almost proportionally to the FRP volumetric ratio.

The effect of the number of CFRP layers on MSC specimens is relatively moderate compared to NSC specimens. The enhancement in the axial strength is reduced and varies roughly from 16% to 35%, whereas the axial strain at peak stress displaying an increase on average from 32% to 106%.

Regarding HSC specimens, the effect of the number of CFRP layers is relatively low compared to previously. In this situation, the confinement pressure is activated at higher load (around 80% of the ultimate value). Consequently, the enhancement in the axial strength is reduced and varies from 9% to 24%, whereas the axial strain at peak stress undergoes a significant reduction displaying an increase on average from 2% to 97%, as illustrated in Tables 4, 5 and 6.

It should be emphasized that the presence of quite sharp corners in all tested CFRP jacketed columns produced a cutting effect on confining sheets and hence affected the rate of enhancement in their axial strength and ductility.

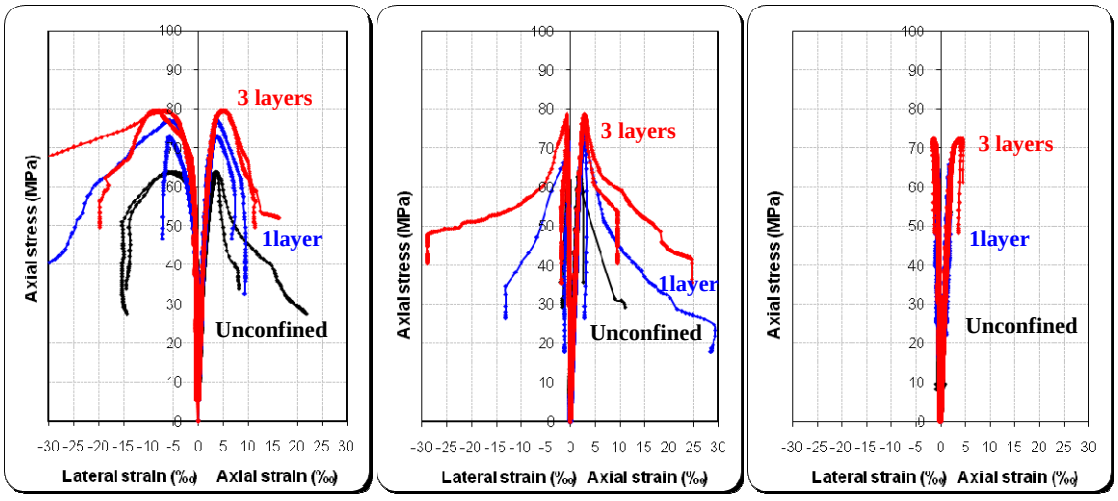

(a) RCIII.x series (b) RCIII.y series (c) RCIII.z series

Fig. 8 Stress strain curves of HSC CFRP-confined specimens

5.3 Effect of unconfined concrete strength

To investigate the effects of concrete quality, different concrete strengths (26, 50 and 62 MPa) have been used. Fig. 9 shows the increase in compressive strength versus the unconfined concrete strength f'_{co} for plain and RC specimens confined with one and three CFRP layers. It is evident that as the unconfined concrete strength increases, the confinement effectiveness decreases. The FRP-wrapped specimens with the least f'_{co} (26 MPa) show the maximum increases in confined strength f'_{cc}. Fig. 10 shows the effect of f'_{co} on the peak strain ε_{cc} of the confined concrete. Test results clearly showed that the confinement effectiveness reduces with an increase in the unconfined concrete strength. These Figures also show that strength and strain enhancement was more significant for NSC specimens than for MSC and HSC ones.

This clearly indicates that the effect on the strength and ductility capacities decreases with increasing concrete strength. Mechanical effects of different concrete qualities are also evident in the first branch of the curves, where stronger concrete shows higher stiffness with respect to concrete with lower strength.

5.4 Effect of slenderness ratio

The comparison of results recorded for the slenderness ratio varying from 2 to 7.14 shows for NSC wrapped RC specimens a moderate decrease in the axial strength and an important reduction in the axial deformation (Figs. 11 and 12). Each point on the graph represents the average value of two specimens tested under compression. However, in the case of MSC and HSC jacketed specimens, the strength was almost not affected whereas the ductility undergoes a moderate decrease (except for specimen SRIII.z.3L where an increase was observed in ε_{cc}).

This moderate decrease of ductility may be explained by the late activation of the confinement pressure which occurred at higher load (around 80% of the ultimate value). The measurement of deformations at the mid-height of the columns can also explain this reduction, because the stress distribution along the slender specimens is not the same. The mode of failure of these slender specimens confirms the stress concentration at the ends.

On overall, the efficiency of the confinement provided by composite wraps was greatly affected by the premature damage of the CFRP fabric at the sharp column corner.

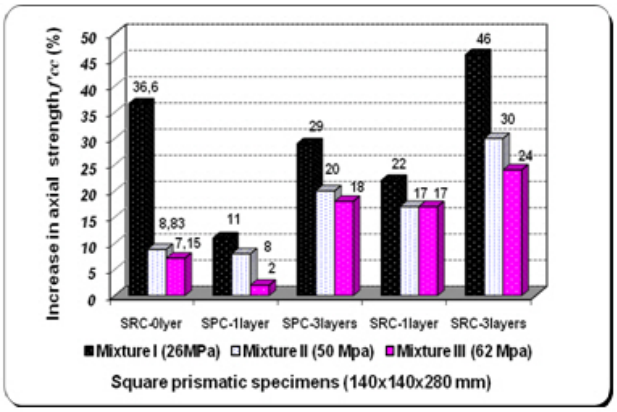

Fig. 9 Effect of unconfined strength of concrete on peak stresses

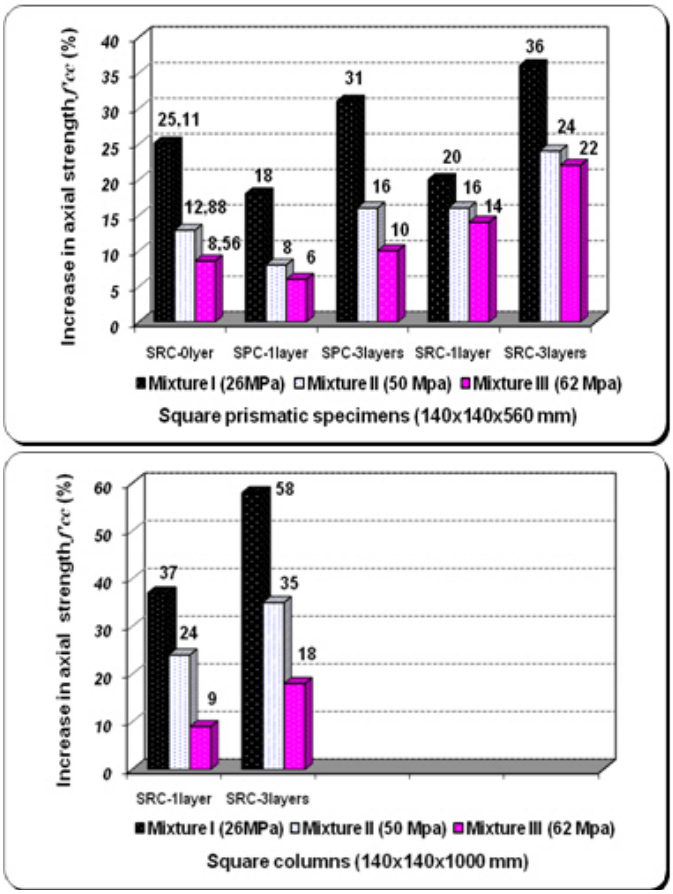

Fig. 9 Continued

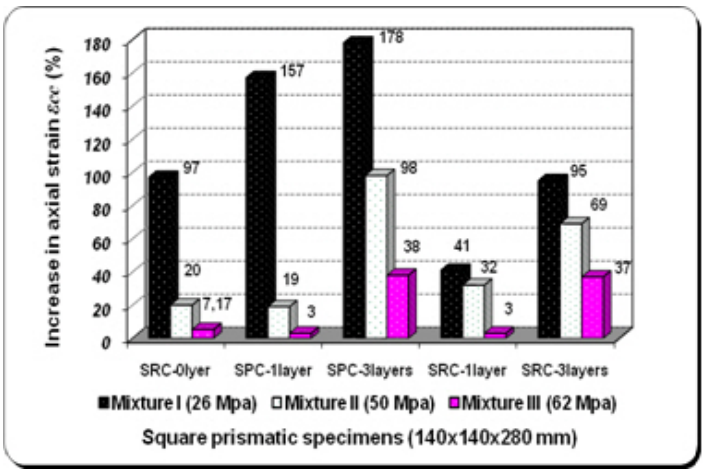

Fig. 10 Effect of unconfined strength of concrete on peak strains

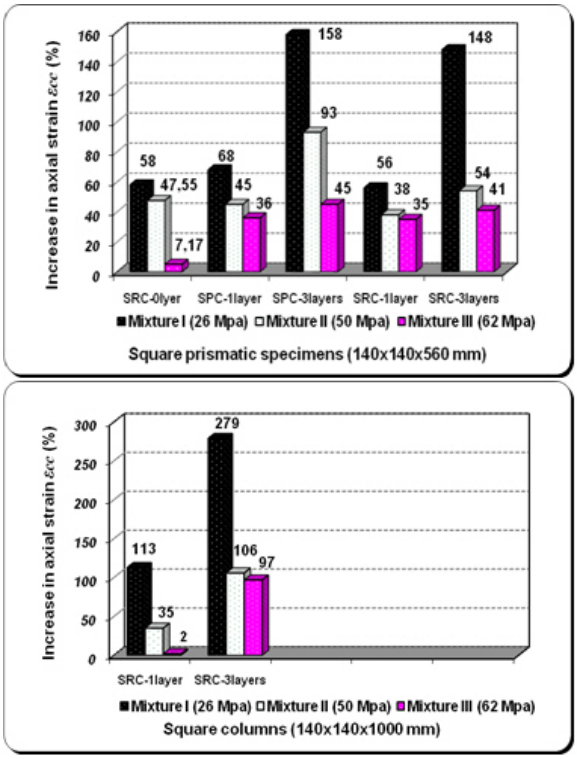

Fig. 10 Continued

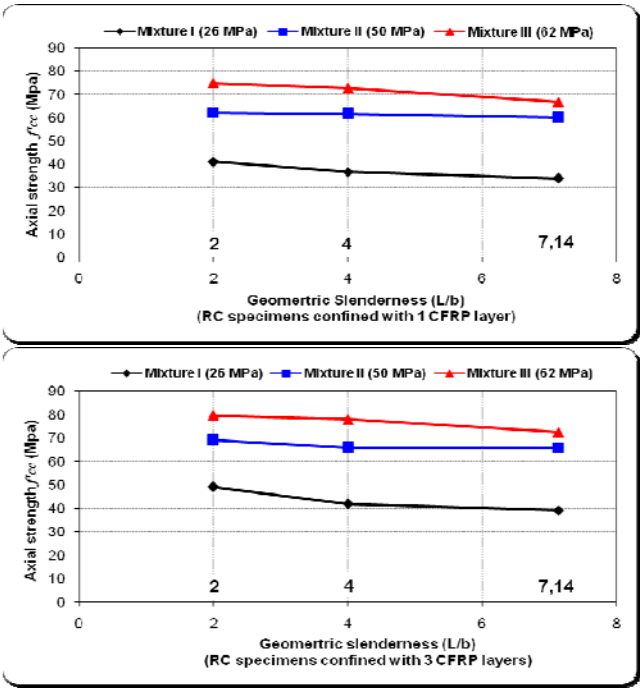

Fig. 11 Effect of slenderness ratio on peak stresses

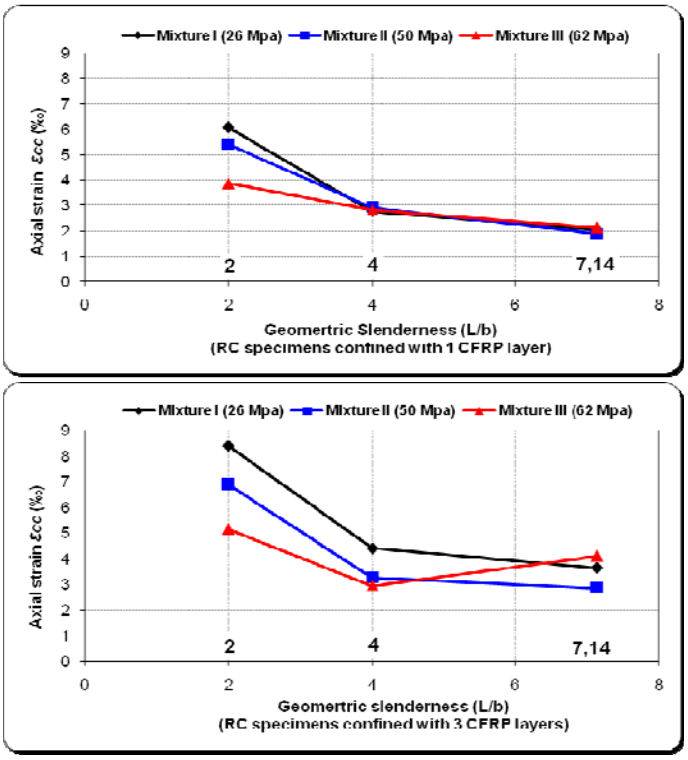

Fig. 12 Effect of slenderness ratio on peak strains

6. Proposed model of FRP-confined square columns

The average hoop strain in FRP at rupture in FRP wrapped concrete can be much lower than the FRP material ultimate tensile strain from flat coupon tests, indicating the assumption that FRP ruptures when the FRP material tensile strength reached is not valid in the case of concrete confined by wrapped FRP. Based on this observation, a new peak stress formula for FRP-confined square concrete columns must be based on the actual hoop rupture strain of FRP rather than the ultimate material tensile strain.

6.1 Compressive strength

6.1.1 The effective lateral confining pressure

The effective lateral confining pressure f'_l can be defined as a function of the shape (Lam and Teng 2003, Campione and Miraglia 2003, among others) through the use of a confinement effectiveness coefficient k_e as

$$f'_l = k_e \, f_l \tag{3}$$

were f_l is the lateral confining pressure provided by an FRP jacket and can be evaluated using Eq. (1), with the columns diameter d replaced by the diagonal length of the square section. f_l now becomes an equivalent confining pressure provided by the FRP jacket to an equivalent circular

columns. On the other hand, the effective FRP strain coefficient η' is defined as the ratio of the FRP tensile hoop strain at rupture in the square column tests ($\varepsilon_{h,rup}$) to the ultimate tensile strain from FRP tensile coupon tests (ε_{fu})

$$\eta' = \frac{\varepsilon_{h,rup}}{\varepsilon_{fu}} \tag{4}$$

The effective FRP strain coefficient represents the degree of participation of the FRP jacket, and the friction between concrete and FRP laminate. Type bond, geometry, FRP jacket thickness, and type of resin affect the effective FRP strain coefficient. From representative experimental results η' was 68 % on average for square bonded jackets.

Based on these observations, the effective equivalent lateral confining pressure f_l for square section is given by

For square section $$f_l = \frac{2\ t_{frp}\ E_{frp}\ \varepsilon_{h,rup}}{\sqrt{2}\ b} = \frac{2\ t_{frp}\ E_{frp}\ \eta'\varepsilon_{fu}}{\sqrt{2}\ b} \tag{5}$$

For square section with round corners $$f_l = \frac{2\ t_{frp}\ E_{frp}\ \varepsilon_{h,rup}}{\sqrt{2}\ b - 2Rc\ \left(\sqrt{2}-1\right)} = \frac{2\ t_{frp}\ E_{frp}\ \eta'\varepsilon_{fu}}{\sqrt{2}\ b - 2Rc\ \left(\sqrt{2}-1\right)} \tag{6}$$

6.1.2 Confinement effectiveness coefficient "k_e"

For the determination of the effectiveness factor k_e it can be assumed that, in the case of a circular cross-section, the entire concrete core is effectively confined, while, for the square section there is a reduction in the effectively confined core that can be assumed, analogously with the case of concrete core confined by transverse steel stirrups (Mander *et al*. 1988), in the form of a second-degree parabola with an initial tangent slope of 45°. For a square section wrapped with FRP (Fig. 1(a)) and with corners rounded with a radius Rc, the parabolic arching action is again assumed for the concrete core where the confining pressure is fully developed. Unlike a circular section, for which the concrete core is fully confined, a large part of the cross-section remains unconfined (Lam and Teng 2003, Campione and Miraglia 2003). Based on this observation, it is possible to obtain the area of unconfined concrete A_u, as follows

$$A_u = 4\left(\frac{b^2}{6}\right) = \frac{2\ b^2}{3} \quad \text{(for square section)} \tag{7}$$

$$A_u = 4\left(\frac{b'^2}{6}\right) = \frac{2\ b'^2}{3} \quad \text{(for square section with round corners)} \tag{8}$$

The confinement effectiveness coefficient k_e is given by the ratio of the effective confinement area A_e to the total area of concrete enclosed by the FRP jacket, A_c, as follows

$$k_e = \frac{A_e}{A_c} = \frac{\left(A_c - A_u\right)}{A_c} = 1 - \frac{A_u}{\left(A_g - A_s\right)} = 1 - \frac{A_u}{A_g\ \left(1-\rho_{sc}\right)} \tag{9}$$

Where A_g is the gross area of column section, and ρ_{sc} is the cross-sectional area ratio of longitudinal steel.

By substituting the expression (5) or (6) into (7), the confinement effectiveness coefficient k_e is therefore given by

$$k_e = 1 - \frac{2\ b^2}{3A_g\ (1-\rho_{sc})} \text{ (for square section)} \tag{10}$$

$$k_e = 1 - \frac{2\ b'^2}{3A_g\ (1-\rho_{sc})} \text{ (for square section with round corners)} \tag{11}$$

6.1.3 Proposed equation

Base on the linear equation proposed by Richart *et al*. (1929) for uniformly confined concrete, the proposed model employs similar approach with some modifications accounting for the effect of the shape (by introducing a confinement effectiveness coefficient k_e) , effective FRP strain and effective confinement (by introducing the effective FRP strain coefficient η'). The compressive strength of a square FRP-confined concrete column is proposed to be a simple modification of the Benzaid *et al*. (2010) model by the introduction of a confinement effectiveness coefficient denoted k_e. Thus

$$\frac{f'_{cc}}{f'_{co}} = 1 + k_1 k_e \frac{f_l}{f'_{co}} \tag{12}$$

Where ($k_e\ f_l / f'_{co}$) is the effective confinement ratio. The coefficient k_1 was taken as 1.60, which was suggested for uniformly confined concrete (Compione and Miraglia 2003). Considering the known values of the product of the parameters k_1 and k_e as found from expression (12) for the tested specimens of this work, the values of k_e were deduced, and were on average equal to 0.36. Finally, the equation proposed for the confined concrete strength is

$$f'_{cc} = f'_{co} + 0.58\ f_l \tag{13}$$

6.2 Axial strain at peak stress

Similarly to the compressive strength, the axial strain at peak stress is proposed to be given by the following equation in which a different confinement effectiveness coefficient, k_{e2}, is introduced

$$\frac{\varepsilon_{cc}}{\varepsilon_{co}} = 2 + k_2 k_{e2} \left(\frac{f_l}{f'_{co}} \right) \tag{14}$$

In Eq. (14), f_l is the confining pressure in an equivalent circular column given by Eq. (15) for square section, while $k_2 = 5.55$ and $k_{e2} = 0{,}72$. The equation proposed for the axial strain is

$$\varepsilon_{cc} = \varepsilon_{co} \left[2 + 4 \left(\frac{f_l}{f'_{co}} \right) \right] \tag{15}$$

6.3 Comparison between proposed model and existing test data

Tables 7 and 8 show comparisons between the predictions of the proposed model and the experimental results collected from other studies (Demer and Neale 1994, Lam and Teng 2003, Rochette 1996, Benzaid 2010) for the compressive strength and the axial strain at peak stress of FRP-confined concrete in square sections. Clearly, the present model is more accurate in predicting the compressive strength but less accurate in predicting the axial strain. Accurate predictions of the axial strain are an issue that will require a great deal of further research.

Table 7 Performance of proposed model: compressive strength

Specimen code	*FRP type*	f'_{co} *(MPa)*	t_{frp} *(mm)*	E_{frp} *(GPa)*	ε_{fu} *(‰)*	*b (mm)*	*Rc (mm)*	*d (mm)*	f_l *(MPa)*	f'_{cc} *(MPa)*	$f'_{cc\ .théo}$	$f'_{cc.\ théo}/f'_{cc.exp}$
Demers and Neale (1994)												
-	CFRP	32.3	0.9	25	15.2	152	5	210.81	2.20	34.1	33.57	0.98
-	CFRP	42.2	0.9	25	15.2	152	5	210.81	2.20	45.99	43.47	0.94
-	CFRP	42.2	0.9	25	15.2	152	5	210.81	2.20	45.7	43.47	0.95
Lam and Teng (2003)												
$S1R_{15}$	CFRP	33.7	0.165	257	17.58	150	15	199.70	5.07	35	36.64	1.04
$S2R_{15}$	CFRP	33.7	0.33	257	17.58	150	15	199.70	10.15	50.4	39.58	0.78
Rochette (1996)												
2B	CFRP	42	0.9	82.7	15	152	5	210.81	7.20	39.4	46.17	1.17
2D1	CFRP	42	0.9	82.7	15	152	25	194.24	7.81	42.1	46.53	1.10
2D2	CFRP	42	0.9	82.7	15	152	25	194.24	7.81	44.1	46.53	1.05
2G1	CFRP	42	0.9	82.7	15	152	38	183.48	8.27	47.3	46.79	0.98
2G2	CFRP	42	0.9	82.7	15	152	38	183.48	8.27	50.4	46.79	0.92
2C	CFRP	43.9	1.5	82.7	15	152	5	210.81	12.00	44.1	50.86	1.15
2E	CFRP	43.9	1.2	82.7	15	152	25	194.24	10.42	50.8	49.94	0.98
6A	AFRP	43	1.26	13.6	16.9	152	5	210.81	1.86	50.8	44.08	0.86
6D	AFRP	43	5.04	13.6	16.9	152	5	210.81	7.47	54.3	47.33	0.87
6E	AFRP	43	1.26	13.6	16.9	152	25	194.24	2.02	51.2	44.17	0.86
6F	AFRP	43	2.52	13.6	16.9	152	25	194.24	4.05	51.2	45.35	0.88
6G	AFRP	43	3.78	13.6	16.9	152	25	194.24	6.08	53.2	46.52	0.87
6H	AFRP	43	5.04	13.6	16.9	152	25	194.24	8.11	55.2	47.70	0.86
6I	AFRP	43	2.52	13.6	16.9	152	38	183.48	4.29	50.9	45.49	0.89
6J	AFRP	43	3.78	13.6	16.9	152	38	183.48	6.43	52.7	46.73	0.88
Benzaid (2010)												
$P300\text{-}R0\text{-}1P_1$	GFRP	54.8	1.04	23.8	21.2	100	0	141.42	5.04	54.5	57.72	1.05
$P300\text{-}R0\text{-}1P_2$	GFRP	54.8	1.04	23.8	21.2	100	0	141.42	5.04	56.6	57.72	1.01
$P300\text{-}R0\text{-}1P_3$	GFRP	54.8	1.04	23.8	21.2	100	0	141.42	5.04	57.2	57.72	1.00
$P300\text{-}R8\text{-}1P_1$	GFRP	54.8	1.04	23.8	21.2	100	8	134.79	5.29	58.85	57.87	0.98
$P300\text{-}R16\text{-}1P_1$	GFRP	54.8	1.04	23.8	21.2	100	16	128.16	5.56	60.56	58.02	0.95
									Average:			0.96
									Standard deviation:			0.09
									Coefficient of variation (%):			10.0

Table 8 Performance of proposed model: axial strain

Specimen code	*FRP type*	ε_{co}	$\varepsilon_{cc,exp}$	$k_2\, k_{e2}$	$\varepsilon_{cc,theo}$	$\varepsilon_{cc,theo} / \varepsilon_{cc,exp}$
Demers and Neale (1994)						
1	CFRP	0.002	0.004	4	0.0045	1.13
2	CFRP	0.002	0.0035	4	0.0044	1.26
3	CFRP	0.002	0.0035	4	0.0044	1.26
Lam and Teng (2003)						
$S1R_{15}$	CFRP	0.001989	0.004495	4	0.0051	1.15
$S2R_{15}$	CFRP	0.002	0.0087	4	0.0064	0.73
Rochette (1996)						
2B	CFRP	0.003	0.0069	4	0.0080	1.16
2D1	CFRP	0.003	0.0094	4	0.0082	0.87
2D2	CFRP	0.003	0.0089	4	0.0082	0.92
2G1	CFRP	0.003	0.0108	4	0.0083	0.77
2G2	CFRP	0.003	0.0116	4	0.0083	0.72
2C	CFRP	0.003	0.0102	4	0.0092	0.90
2E	CFRP	0.003	0.0135	4	0.0088	0.65
6A	AFRP	0.003	0.0106	4	0.0065	0.61
6D	AFRP	0.003	0.0124	4	0.0080	0.65
6E	AFRP	0.003	0.0079	4	0.0065	0.83
6F	AFRP	0.003	0.0097	4	0.0071	0.73
6G	AFRP	0.003	0.011	4	0.0076	0.69
6H	AFRP	0.003	0.0126	4	0.0082	0.65
6I	AFRP	0.003	0.0096	4	0.0071	0.74
6J	AFRP	0.003	0.0118	4	0.0077	0.66
Benzaid (2010)						
$P300\text{-}R0\text{-}1P_1$	GFRP	0.0025	0.0088	4	0.0059	0.67
$P300\text{-}R0\text{-}1P_2$	GFRP	0.0025	0.0090	4	0.0059	0.65
$P300\text{-}R0\text{-}1P_3$	GFRP	0.0025	0.0098	4	0.0059	0.60
$P300\text{-}R8\text{-}1P_1$	GFRP	0.0025	0.0091	4	0.0059	0.65
$P300\text{-}R16\text{-}1P_1$	GFRP	0.0025	0.0098	4	0.0060	0.61
			Average:			0.81
			Standard deviation:			0.21
			Coefficient of variation (%):			26.3

7. Conclusions

In this paper an experimental program has been presented whose aim is to study the axial compression behavior of plain concrete and reinforced concrete columns of a square cross-section confined externally with CFRP sheets. The following conclusions can be drawn from the study:

• The failure of all CFRP wrapped specimens occurred in a sudden and explosive way preceded by typical creeping sounds. For short specimens (L/a = 2), the fiber rupture starts mainly in their central zone, then propagates towards both ends. Regarding slender specimens, the collapse was

mostly concentrated in their upper or lower regions, indicating that the greater the slender ratio, the smaller the area of CFRP ruptured;

• On overall, CFRP strengthened specimens showed a typical bilinear trend with a transition zone. The first zone is essentially a linear response governed by the stiffness of the unconfined concrete. No distinct post behavior is observed as the slenderness ratio increases and a little reduction is recorded in strength compared to the reduction in ductility.

• Increasing the amount of CFRP sheets produces an increase in the compressive strength of the confined column but with a lower rate compared to that of the deformation capacity which is almost proportional to the CFRP volumetric ratio;

• The increase in strength and strain produced by CFRP confinement for low-strength concrete specimens is greater than that for high-strength concrete specimens. Therefore, the effect of CFRP confinement on the bearing and deformation capacities decreases with increasing concrete strength;

• The effect of increasing the slenderness ratio results in a decrease of the strengthening effect on strength and ductility. The rate of decrease is more important for NSC specimens.

Further work is required to verify the applicability of the proposed model over a wider range of geometric and material parameters, to improve their accuracy (particularly that of the axial strain at peak stress) and to place their on a clear mechanical basis. Both additional tests and theoretical investigation are needed.

Acknowledgments

Authors thankfully acknowledge Sika France S.A, Saint Grégoire – Rennes, for their support for providing the fiber-reinforced polymer materials.

References

Al-Salloum, Y.A. (2007), "Influence of edge sharpness on the strength of square concrete columns confined with frp composite laminates", *Composite Part B*, **38**, 640-650.

Almusallam, T.H. (2007), "Behavior of normal and high-strength concrete cylinders confined with E-glass/epoxy composite laminates", *Composites part B*, **38**, 629-639.

Benzaid, R., Chikh, N.E. and Mesbah, H. (2008), "Behaviour of square concrete columns confined with GFRP composite wrap", *J. Civil Eng. Manag*., **14**(2), 115-120.

Benzaid, R., Chikh, N.E. and Mesbah, H. (2009), "Study of the compressive behavior of short concrete columns confined by fiber reinforced composite", *Arab. J. Sci. Eng*., **34**(1B), 15-26.

Benzaid, R., Mesbah, H. and Chikh, N.E. (2010), "FRP-confined concrete cylinders: axial compression experiments and strength model", *J. Reinf. Plast. Compos.*, **29**(16), 2469-2488.

Benzaid, R. (2010), "Contribution à l'étude des matériaux composites dans le renforcement et la réparation des eléments structuraux linéaires en béton", Thèse de Doctorat, INSA de Rennes, France. (In French)

Cusson, D. and Paultre, P. (1995), "Stress-strain model for confined high-strength concrete", *ASCE J. Struct. Eng.*, **121**(3), 468-477.

Cole, C. and Belarbi, A. (2001), "Confinement characteristics of rectangular FRP jacketed RC columns", *Proceedings of the Fifth International Symposium on Fiber Reinforced Polymer for Reinforce Concrete Structures (FRPRCS-5)*, Cambridge, 823-832.

Campione, G. and Miraglia, N. (2003), "Strength and strain capacities of concrete compression members reinforced with FRP", *Cem Concr Compos.*, **25**, 31-41.

Demer, M. and Neale, K.W. (1994), "Strengthening of concrete columns with unidirectional composite sheets", Eds. Mufti, A.A., Bakht, B. and Jaeger, L.G., *Development in Short and Medium Span Bridge Engineering'94*, *Proceedings of the fourth International Conference on Short and Medium Span Bridges*, Canadian society for civil engineering, Montreal, Canada.

Lam, L. and Teng, J.G. (2003), "Design-oriented stress-strain model for FRP-confined concrete in rectangular columns", *J. Reinf. Plast. Compos*., **22**(13), 1149-1186.

Mander, J.B., Priestley, M.J.N. and Park, R. (1988), "Theoretical stress-strain model for confined concrete", *ASCE*, *J. Struct. Eng.*, **114** (8), 1804-1826.

Mirmiran, A., Shahawy, M., Samaan, M. and El Echary, H. (1998), "Effect of column parameters on FRP-confined concrete", *ASCE J. Compos. Constr.*, **2**(4), 175-185.

Matthys, S., Toutanji, H., Audenaert, K. and Taer we, L. (2005), "Axial load behavior of large-scale columns confined with fiber-reinforced polymer composites", *ACI Struct. J*., **102**(2), 258-267.

NF EN ISO 527-1 (1993), *Determination of Tensile Properties of Plastics Materials Part 1: General Principles*, ISO International Standards.

NF EN ISO 527-2 (1993), *Determination of Tensile Properties of Plastics Materials Part 2: Test Conditions for Moulding and Extrusion Plastics*, ISO International Standards.

NF EN ISO 527-5 (1997), *Determination of Tensile Properties of Plastics Materials Part 5: Test Conditions for Unidirectional Fibre-Reinforced Plastic Composites*, ISO International Standards.

Park, R. and Paulay, T. (1975), *Reinforced Concrete Structures*, John Wiley and Sons, N.Y., U.S.A.

Richart, F.E., Brandtzaeg, A. and Brown, R.L. (1929), *The Failure of Plain and Spirally Reinforced Concrete in Compression*, Bulletin No.190, Engineering Experiment Station, University of Illinois, Urbana, USA.

Rochette, P. (1996), "Confinement de colonnes courtes en béton de section carrée ou rectangulaire avec des matériaux composites", Maîtrise Es-Sciences Appliquées, Université de Sherbrooke, Canada. (In French)

Rochette, P. and Labossière, P. (2000), "Axial testing of rectangular column models confined with composites", *ASCE J. Compos. Construct.,* **4**(3), 129-136.

Saadatmanesh, H., Ehsani, M.R. and Li, M.W. (1994), "Strength and ductility of concrete columns externally reinforced with composites straps", *ACI Struct. J.,* **91**(4), 434-447.

Samaan, M., Mirmiran, A. and Shahawy M. (1998), "Model of concrete confined by fiber composites", *ASCE, J. Struct. Eng*., **124**(9), 1025-1031.

Shehata, I.A.E.M., Carneiro, L.A.V. and Shehata, L.C.D. (2002), "Strength of short concrete columns confined with CFRP sheets", *RILEM Mater. Struct*., **35**, 50-58.

Wu, G., Lu, Z.T. and Wu, Z.S. (2006), "Strength and ductility of concrete cylinders confined with FRP composites", *Construct. Build. Mater*., **20**, 134-148.

Yang, X., Nanni, A. and Chen, G. (2001), "Effect of corner radius on the performance of externally bonded FRP reinforcement", *Proceedings of the Fifth International Symposium on Fiber Reinforced Polymer for Reinforce Concrete Structures (FRPRCS-5)*, Cambridge, 197-204.

Youssef, M.N., Feng, M.Q. and Mosallam, A.S. (2007), "Stress-strain model for concrete confined by FRP composites", *Composites: Part B*, **38**, 614-628.